 Vol. **47**, No. 4, pp. 565–579 (2022), doi: 10.24425/aoa.2022.142903

Review Paper

Electron Properties Investigation of the Near-Surface Region in Crystalline Semiconductors Using the Transverse Acoustoelectric Effect

Tadeusz PUSTELNY

Department of Optoelectronics, Silesian University of Technology
Gliwice, Poland; e-mail: tpustelny@polsl.pl

(*received September 7, 2022; accepted October 31, 2022*)

The paper presents the acoustoelectric phenomenon in a layered structure: piezoelectric waveguide – semiconductor. The publication presents an original acoustic method for determining the electrical and electron parameters of the subsurface area in crystalline semiconductors. The method is based on the so-called transverse acoustoelectric effect realized in a layer system: piezoelectric waveguide with Rayleigh surface acoustic wave – semiconductor. The paper discusses the physical foundations of the transverse acoustoelectric effect in the piezoelectric – semiconductor layer system, taking into account the distinctness of the physical properties of the semiconductor near-surface region in relation to its volumetric properties. The work covers many experimental studies of the near-surface region of semiconductors. The original method was presented to determine such surface parameters as: surface potential, surface conductivity, mobility of carriers in the subsurface area, life time of charge carriers in surface states. By means of the acoustic method the following semiconductors have been extensively tested: indium phosphide InP and gallium phosphide GaP. These semiconductors are one of the main semiconductors of group III-V, which are the basis of modern photonics, optoelectronics as well as integrated optics. The work also includes an analysis of the measurement possibilities of the developed acoustic method and its limitations, as well as an analysis of the accuracy of the obtained values of the parameters of the subsurface area of crystalline semiconductors.

Keywords: surface acoustic wave; acoustoelectric effects; electron properties of semiconductors.

Copyright © 2022 The Author(s). This is an open-access article distributed under the terms of the Creative Commons Attribution-ShareAlike 4.0 International (CC BY-SA 4.0 https://creativecommons.org/licenses/by-sa/4.0/) which permits use, distribution, and reproduction in any medium, provided that the article is properly cited. In any case of remix, adapt, or build upon the material, the modified material must be licensed under identical terms.

1. Introduction. The near-surface region of semiconductors

The study of electronic processes taking place on the surface of semiconductors is one of the areas where the interests of many directions of modern science and technology are combined. Surface phenomena play an important role in semiconductor electronics, especially in the part that uses miniaturized elements and low-power electronics systems. The characteristics of semiconductor systems are largely determined by the phenomena in the near-surface layer (Many *et al.*, 1979; Peka, 1987; Wojas, 1995). The physic-chemical structure of the surface in microelectronics plays a decisive role: in systems with a high degree of integration and in high-frequency systems (Wolf, 1979; Holmes, 1987; Weisbuch *et al.*, 1991; Red, Snitko, 1994).

The importance of studying surface processes is not limited to practical applications. Researches in the field of surface physics are also important for cognitive reasons. It is more convenient to study a number of basic physical phenomena in a semiconductor not in the volume of the semiconductor, but on its surface. Examples include the study of elementary acts of trapping and recombination of non-equilibrium charge carriers. When studying these processes on the surface, it is relatively easy to change the position of the Fermi level in relation to the trap levels, on one and the same sample (Sze, 1995). Surface physics quickly developed into one of the large fields of solid state physics.

In the group of methods of studying the surface of semiconductors, the methods of studying the electronic properties and electrical properties of this surface have an important position. Compounds of elements group III and V of the periodic table play an important role in electronic technology (Macinnes *et al.*, 1993). Due to their interesting properties, group III-V materials are widely used in photonics and laser technologies (Sze, 1995).

The properties of the real surface of group III-V semiconductors are a direct consequence of the electronic, structural, and chemical heterogeneity of this surface. The aim of the author's many years of research was to develop a new acoustic method for studying the electronic properties of semiconductor surfaces, including group III-V semiconductors (Pustelny, 1995; Pustelny, Pustelny, 2006; 2008; 2009; Pustelny *et al.*, 2008).

The development of the method and the research of the real surface of group III-V semiconductors required solving various problems in the field of acoustics, physics of semiconductor surfaces, as well as the technology of preparation of semiconductor substrates. Group III-V semiconductors belong to the so-called complex two-component semiconductors. They are composed of the elements of the main groups: the third (B, Al, Ga, In) and the fifth (N, P, As, Sb). Their crystal structures are that of a zinc blende (Wolf, 1979).

Complex two-component semiconductors differ from simple semiconductors in the heteropolar nature of network bonds, the non-parabolic shape of the conductivity band, a simple forbidden bond, and the possibility of deviations from stoichiometry. Compared to other complex semiconductors, group III-V semiconductors are characterized by relatively small deviations from the stoichiometry. Their most important admixtures (they are group II, IV, VI atoms) are built into nodes of the crystalic lattice (Sze, 1995). Consequently, III-V compounds combine the advantages of simple semiconductors with other interesting properties, first of all – optical properties, mainly in the field of radiation generation in the UV, VIS, and IR range (Weisbuch *et al.*, 1991).

The limitation of the thickness dimensions of semiconductor samples, their surface treatment and contact with the surrounding atmosphere generate energetical surface states in them. Geometrically, the surface states in semiconductor are located in the near-surface region. The energy levels which they create are usually in the forbidden band. Various types of defects are the reasons for the occurrence of surface states. The main defect of the real crystal is its finite size – the interruption of the periodicity of the infinite crystal lattice of the ideal crystal. For group III-V semiconductors, obtaining a surface close to atomically pure surface is a difficult task (Wojas, 1995). The reason for this is the high chemical activity of surface atoms with unsaturated bonds, as well as the natural tendency to surface non-stoichiometry [1 0 0], [1 1 0], and [1 1 1]. The crystallographic planes used in the technology are characterized by the following properties:

- the [1 0 0] plane is built of atoms of one type, each atom is bound by two bonds with atoms of the other type, of the underlying layer, and two bonds are broken;
- the [1 1 0] plane contains the same number of atoms III and V of the group, each of the atoms is bonded with one bond to the underlying layer, two bonds to atoms of the first layer, the fourth bond is free (plane [1 1 0] is the cleavage plane);
- the [1 1 1] plane can be of both the first and the second type, where each atom of the surface layer has one free bond.

The real surface of the crystal of this group is covered with a layer of chemical compounds formed as a result of reactions between surface atoms and the surrounding medium (MacInnes *et al.*, 1993).

The transition of free carriers to surface states causes that the subsurface area is not electrically neutral. The semiconductor surface is electrically charged. There is an electrical potential (surface potential) associated with this charge. It disturbs the energy of charge carriers near the surface. In the energy diagram, the existence of the subsurface layer is expressed in the change in the position of the boundaries of the bands in the area of the surface charge in relation to the Fermi level. The depth of the near-surface region is of the order of the effective length of the Debye shielding radius L_D (Wojas, 1995).

Electron states occurring in the subsurface area can be divided into free ionic states in the oxide layer and slow and fast electronic states in the semiconductor subsurface area. The division criterion is the speed which the charge carriers interact with them. The mobility of carriers in the near-surface region is generally different from that in the depth of the semiconductor. This is related to the additional scattering of the carriers on the surface. Fast surface states are the centres of recombination on the real surface of a semiconductor. Recombination of charge carriers through the surface levels can significantly affect the process of restoring the balance of charge carrier distribution. A semiconductor, in which the surface recombination is also observed, is characterized by a different effective lifetime of the charge carriers τ_{ef}.

In the group of III-V semiconductors, four crystals have found practical application in the technology of electronic components: gallium arsenide, gallium phosphide, indium phosphide, and indium arsenide (GaAs, GaP, InP, InAs). Gallium arsenide is the most widely used. It is also the most studied and best-known material. Group III-V semiconductors are characterized by a number of specific volumetric properties related to the mixed, ion-covalent nature of the chemical bond. The surface electronic properties occupy an intermediate place between the properties of the surface states of covalent semiconductors and the states of crystals with ionic bonds.

The electron heterogeneity of the actual semiconductor surface is related to the presence of broken surface bonds, produced as a result of breaking the periodicity of the crystal lattice on the crystal surface.

On the other hand, the structural heterogeneity of the actual semiconductor surface is related to the presence of macroscopic and microscopic structural defects on it. Macroscopic structural defects, which include, inter alia, surface faults, cracks, scratches, and post-etch cavities are caused by the technological treatment of the crystal surface. The chemical inhomogeneity of the actual semiconductor surface is the result of the unavoidable adsorption on the crystal surface, as a result of its contact with the environment other than perfect vacuum, of the active ingredients of both chemical solutions during the mechanical and chemical treatment of the actual semiconductor surface, and always surrounding the crystal surface, determined gaseous atmosphere.

Classically, the methods of studying the surface of semiconductors can be divided into electrophysical methods, photoelectric methods, electromagnetic methods, spectroscopic methods (Peka, 1987; Tabib-Azar, 1998). It can be seen that among the methods of studying semiconductor surfaces, there are no methods for dynamically determining the electrical and electronic values of the surface parameters of semiconductors. The only dynamic method is the high frequency field effect method. However, its frequency range is limited to only a few dozen MHz. When it is necessary to operate electronic circuits in the higher frequency, the high-frequency acoustic method (in the range of hundreds of MHz and even GHz) can be used in the study of electron properties of semiconductor surfaces.

The generation and detection of signals in the range of high and very high frequencies have significant utilitarian aspects: better and faster internet, better information technologies, more efficient and faster processors, and the possibility of realization processes in the so-called real time. Material research in the field of high frequencies also has an essential cognitive aspect – they enable, among others, studies of physical effects and phenomena at the quantum level, including investigation in molecular and quantum acoustics.

2. Acoustoelectric effects

Interest in using of the phenomenon of surface acoustic wave (SAW) propagation in the structure: piezoelectric waveguide – semiconductor appeared in science in the late seventies of the previous century (Auld, 1973; Gulyaev, 2005; Vanneste, Buhler, 2011; Gustafsson *et al.*, 2014). These phenomena were referred to as acoustoelectric effects. The use of Rayleigh-type surface waves was of particular interest. Some researchers drew attention to the dependence of acoustoelectric interactions on the electron properties of the semiconductor near-surface layer. The influence of electron and electrical properties on the intensity of acoustoelectric interactions in the piezoelectric – semiconductor system and the potential use of these effects in the study of semiconductor surfaces was indicated.

Due to the type of effects used to determine the electronic properties of the near-surface area in semiconductors, acoustic methods can be divided into two groups. The first one includes methods based on the effects related to changes in the parameters of an acoustic wave as a result of its interaction through piezofield with electric charges in a semiconductor (attenuation of a propagating wave and changes in its velocity) (Zhu *et al.*, 2004; Jakubik *et al.*, 2005; Pustelny *et al.*, 2008; Pasternak *et al.*, 2020). The second group includes methods that use the effects generated in a semiconductor under the influence of the field of a propagating wave. We include primarily to them: longitudinal and transverse acoustoelectric phenomena, and acoustomagnetic phenomena (Pustelny, 1997; Rotter *et al.*, 1999; Kapelewski, Lila, 2011; Bury *et al.*, 2003; Samulionis *et al.*, 2004; Hermelin *et al.*, 2011; Elhosni *et al.*, 2016).

2.1. The piezoelectric-semiconductor acoustic layered structure

In a solid body of limited size, in addition to acoustic volume waves, surface acoustic waves can propagate. The Rayleigh waves play an important role in the group of surface waves. The Rayleigh waves in an isotropic medium are characterized by the existence of two components of mechanical displacements: one in the direction of wave propagation, the other – in the direction perpendicular to the plane of propagation. There may be three components of mechanical displacements in the anisotropic medium. The surface wave penetrates the medium along which it propagates in a distance comparable to the wavelength λ_f. Its velocity V_s is lower than the velocity of the slowest shear wave propagating in this direction in the crystal (Auld, 1973).

In the case when the solid is a piezoelectric, deformations and mechanical stresses of the surface wave are accompanied by an electric field. The external medium into which the electric field associated with the acoustic wave propagating in the piezoelectric penetrates, interacting with this field affects the properties of the propagating wave. The interactions between the electric field associated with a surface wave and the charge carriers in a semiconductor constitute the physical basis of the acoustic method of studying the electronic properties of a semiconductor surface. The electric field of the surface wave penetrating into the semiconductor excites excess carriers in it. It also causes them to drift. In a semiconductor, the electric field associated with the wave and the local changes in the concentration of carriers: n electrons and p holes caused by it, are harmonically variable, in accordance with the variability of the surface wave. The longitudinal compo-

nent of the electric field of a surface wave propagating in the piezoelectric causes the flow of electric current in the semiconductor along the direction of the surface wave – the so-called longitudinal acoustoelectric effect (LAE) (Gulyaev, 2005). The transverse component of this field is responsible for changes in the transverse direction of the distribution of electric charge carriers, in a semiconductor and the formation of an additional electric field in this direction, the so-called transverse acoustoelectric voltage, an effect known in the literature as the transverse acoustoelectric effect (TAE).

Figure 1 shows the acoustoelectric effects: longitudinal acoustoelectric current and transverse acoustoelectric voltage in the piezoelectric-semiconductor layer system.

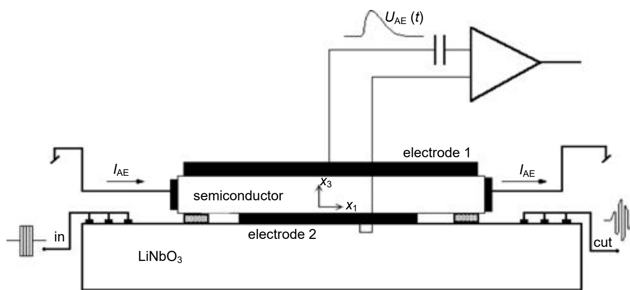

Fig. 1. Acoustoelectric effects in a piezoelectric-semiconductor layered system with an acoustic surface wave, where: I_{AE} is the longitudinal acoustoelectric current; U_{AE} is the transverse acoustoelectric voltage; in, out are input and output acoustic transducers, respectively, and $LiNbO_3$ is the piezoelectric crystal as an acoustics waveguide.

The transverse and longitudinal acoustoelectric effects significantly depend on the electron properties of the near-surface region in the semiconductor, including: concentration of charge carriers (electrons and holes), energy density of recombination, and trap surface states, their location in the forbidden band, the degree of their filling, the curvature of energy bands on the surface, specific so-called surface potential as well as the length of Debye shielding radius, mobility of carriers in the near-surface area, life of carriers in the so-called fast and slow surface states. The author has carried out a thorough theoretical analysis of the transverse acoustoelectric effect. He obtained the following analytical formulas for the amount of the transverse acoustoelectric voltage (TAV) in a layered structure: piezoelectric waveguide with a Rayleigh surface wave – semiconductor (Pustelny, 1997):

$$U_{\mathrm{AE}} = K\frac{\mu_n^2 n_b - \mu_p^2 p_b + n_i \frac{L_i}{L_e}(\mu_n^2 G_n - \mu_p^2 G_p)}{a^*}\frac{\alpha_o S}{\omega \varepsilon_s \varepsilon_o V_s} \tag{1}$$

and

$$\alpha_o = \frac{\omega^2 q[a^*]}{\varepsilon_o^2(\varepsilon_s+\varepsilon_p)^2\omega^2 + q^2[a^*]^2}\frac{K_e \varepsilon_o \varepsilon_p}{V_s}, \tag{2}$$

where

$$a^* = \mu_n n_b + \mu_p p_b + n_i \frac{L_i}{L_e}(\mu_n G_n + \mu_p G_p);$$

U_{AE} is the transverse acoustoelectric voltage; L_e and L_i are Debye effective shielding lengths in volume and in the subsurface area of the semiconductor, respectively; n_b, p_b, n_i are the concentration of electrons and holes in the volume of the tested semiconductor, and in an intrinsic semiconductor; μ_n, μ_p are the mobility of electrons and holes; S is the surface wave power; α_o is the surface wave attenuation (so-called electron wave attenuation); K_e is the electromechanical coupling coefficient; ω, V_s are the surface wave pulsation and velocity; ε_o is the dielectric permittivity of vaccum; ε_s, ε_p are the relative dielectric permittivities of semiconductors and piezoelectrics, respectively; K is the so-called apparatus constant of the test stand.

The mobility of carriers, their concentration, and the length of Debye shielding are expressed through the G_n and G_p functions – the so-called Kingston functions of the 2nd kind for electrons and holes (Many *et al.*, 1979). The Kingston functions are non-elementary integrals containing the surface potential in a semiconductor as a parameter, as well as concentrations and mobility of charge carriers. In theoretical analyzes, they are often expressed in forms of series. For this reason, it should be clearly emphasized that the analytical expressions on the U_{AE} are much more complex than the expressions (1) and (2) would suggest.

2.2. Research motivation

New electronic semiconductor components and systems, including semiconductor lasers and optical radiation sources and detectors based on group III-V and II-VI semiconductors, which have appeared in the last 20–30 years, are a direct consequence of the development of thin film growth epitaxial technology of these semiconductors. The changes in technology have been aimed at precise control of the dynamics of the layer growth processes, improvement of the purity of the obtained layers, extension of the set of usable materials, including sets with a significant difference of lattice constants between the layer and substrate. Hence a necessity has become a repetitive and controlled growth of very thin layers with thicknesses of fractions of nm and sharp, stepping interfaces. The places high demands on the surface preparation process of monocrystalline semiconductor materials. It also places high demands on the metrological technics with which the electronic and electrical properties of the surfaces are studied. A completely separate matter are researches on the development of SAW structures for gas sensors based on nanolayers and nanostructures of complex and organic semiconductors (Jakubik *et al.*, 2005; Urbańczyk *et al.*, 2011; Hejczyk *et al.*, 2015; Hejczyk, Pustelny, 2020) and graphene and oxide graphene (Pustelny *et al.*,

2013; Zheng, Xu, 2011; Drewniak *et al.*, 2013). In sensor nanostructures, their sensitivity to the selected gaseous environment, but also the speed of reaction to the presence of the detected gas in the gas mixture (often in the air atmosphere) and the speed of the so-called process of sensor detoxification, is largely determined by the physicochemical properties of the surface. Practical applications of semiconductor nanostructures in sensor technology give the study of semiconductor surfaces a new, unique role.

This paper presents the results of theoretical and experimental studies of two semiconductors: indium phosphide InP and gallium phosphide GaP. These materials play an important role in modern photonics, optoelectronics, optics, and integrated optics.

In gallium phosphide GaP relative dielectric permittivity is $\varepsilon_s \approx 11$ at room temperature. In the visible range, its refractive index varies between $n \approx 3.2$ and 5.0 which is higher than in most other semiconducting materials. In the optic transparent range, its index is higher than almost any other transparent material, including gemstones (such as diamonds) as well as non-oxide crystals (such as zinc sulphide). Gallium phosphide has been used in the manufacture of red, orange, and green light-emitting diodes (LEDs) with low to medium brightness for several dozen years. It is used standalone or together with gallium arsenide phosphide. LEDs based on pure GaP emit green light at a wavelength of 555 nm. Nitrogen-doped GaP emits yellow-green (565 nm) light, zinc oxide doped GaP emits red (700 nm) (Wolf, 1979). Gallium phosphide is transparent for yellow and red light, therefore GaAsP-on-GaP LEDs are more efficient than GaAsP-on-GaAs.

The application fields of InP splits up into three main areas. It is used as the basis for: optoelectronic components, high-frequency electronics, and photovoltaics.

InP has a direct bandgap, making it useful for optoelectronics devices like laser diodes. It is used as a substrate for epitaxial indium gallium arsenide based optoelectronic devices.

There is still a vastly under-utilized, yet technically exciting zone in the electromagnetic spectrum between microwaves and infrared, often referred to as terahertzes. Electromagnetic waves in this range possess hybrid properties – they show high-frequency and optical characteristics simultaneously. InP based components unlock this spectral range for important new applications. InP is used in high-power and high-frequency electronics because of its superior electron mobility with respect to the more common semiconductors as silicon and gallium arsenide. It was used with indium-gallium-arsenide to make a record breaking pseudomorphic heterojunction bipolar transistor that could operate at some hundred GHz.

Indium phosphide is used as a major technological material for manufacturing photonic integrated circuits for the optical telecommunications industry to enable wavelength-division multiplexing applications.

The information on GaP and InP presented above shows that the study of the subsurface area of these materials, apart from the scientific and cognitive aspect, also has an important utilitarian aspect.

3. Experimental research

The author has carried out a theoretical analysis of the possibility of using the acoustoelectric effect to determine the parameters of the subsurface area in semiconductors. He developed:

- the methodology of experimental determination of surface parameters in group III-V semiconductors from measurements of acousto-electron interactions in the acoustic system: piezoelectric waveguide – semiconductor;
- the research stand;
- the method of determining the surface potential in semiconductors;
- the method of determining the concentration of carriers in the near-surface area;
- the method of determining the electrical conductivity in this area;
- the method of determining the life time of minority carriers;
- the method of determining the mobility of carriers on a surface.

The study investigated the influence of surface preparation and treatment technology on the values of determined surface parameters. The semiconductor surfaces were investigated for the following processing methods:

- grinding with grinding powders of various granularity;
- polishing with corundum powders and diamond paste;
- chemical etching with HF and HNO_3 acid;
- washing and soaking in acetone, benzene, toluene, methyl alcohol, and deionized water;
- heating of materials in the air atmosphere.

Aging tests were carried out to determine the effect of the surface residence time in the tested atmosphere on the values of the controlled surface parameters. The research was conducted in a wide frequency range (30–300 MHz). The developed technique of testing semiconductors surfaces by the transverse acoustoelectric effect method allows to obtain dynamic values of the determined surface parameters. It gives the possibility of conducting research in the field of high frequencies. In this respect, the developed acoustic method occupies a unique position.

The presented method does not require placing ohmic contacts on the tested semiconductor sample. The process of applying ohmic contacts for group III-V semiconductors is technologically difficult. There is a risk that during its course the electronic properties of the tested surface undergo strong changes. The process of applying ohmic contacts has no influence on the test results obtained with the acoustic method.

3.1. Stand for testing the electronic properties of semiconductor surfaces by the acoustoelectric effect method

The technique of testing semiconductor surfaces by the transverse acoustoelectric effect method in some cases required changes in the properties of the subsurface area. Changes in surface parameters should be controlled changes. They should be reversible – after disappearance of the external factor causing the changes, the surface parameters should return to the baseline values. In the tested semiconductor samples, changes in the electrical and electronic values of surface parameters can be implemented in several ways. First of all, the surface properties can be changed by changing the temperature of the sample. If the temperature changes of a semiconductor sample are not carried out in a vacuum, they are usually irreversible changes. Another method of changing the properties of a surface is its optical excitation (its illumination). Yet another method may be to apply an electric field to the semiconductor. In order to change the properties of the subsurface area, the external electric field should have a direction perpendicular to the tested surface. The method of modifying the surface properties with an electric field is particularly convenient and effective. In a simple way, it allows you to change the values of surface parameters in a wide range.

In the presented own research, the external electric field method was used to control changes in the properties of a semiconductor surface.

The main part of the stand is a layered system: piezoelectric waveguide – tested semiconductor. The idea of the piezoelectric – semiconductor system is shown in Fig. 2.

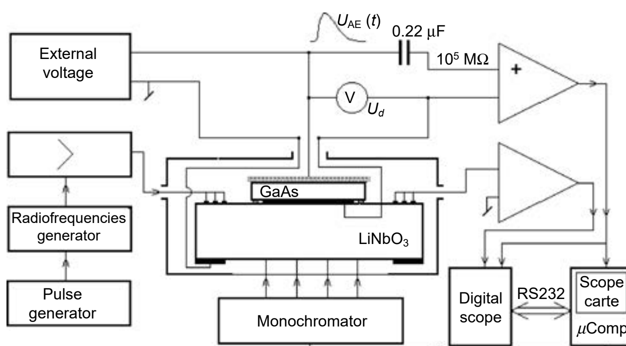

Fig. 2. Measurement system for testing semiconductor surfaces by TAV method.

Lithium niobate $LiNbO_3$ with crystallographic Y cut and Z propagation directions were used as a piezoelectric waveguide. The acoustic surface wave was excited and collected by means of interdigital transducers made with the photolithography method. Two lithium niobate waveguide crystals with transducers of different fundamental frequencies were used.

The developed measuring stand allowed to conduct tests for 11 different frequencies in the range from 30 MHz to 300 MHz (using higher harmonics). Measurement of the transverse acoustic voltage is possible only in a system that uses a periodically excited surface wave. The acoustic surface wave was excited in the form of short, approximately 10 microsecond wave packets with a repetition frequency of several hundred Hz. The electronic parameters of the tested surface were changed by applying an external electric field to the sample, perpendicular to the tested surface. Electric field, in the form of the so-called drift voltage, was applied to the semiconductor using the same electrodes with which the acoustoelectric signal was measured.

The stand for testing the electronic properties of semiconductor surfaces by the acoustoelectric effect method was also presented in (Pustelny, 1997).

3.2. Results of experimental research

The paper presents experimental studies of the subsurface area in indium phosphide InP and gallium phosphide GaP. The studied crystals were produced by:

- Institute of Physics of the Lviv University of Technology (Ukraine) by prof. I. Bobitskij groupe – samples of GaP;
- Institute of Electronic Materials Technology in Warsaw (Łukasiewicz Research Network, Poland) – samples of InP.

GaP samples were doped by Te and Cr:

- crystalline surface orientations: [1 0 0] and [1 1 0];
- concentration of donor admixtures: $N_n < 10^{15}$ cm^{-3};
- mobilities of the carriers in the volume were: μ_n = 110 cm^2/(V·s), μ_p = 75 cm^2/(V·s);
- the bandgap width: ΔE_G = 2.2 eV;
- resistivity: $\rho = 6.4 \cdot 10^5$ [Ω·m];
- permittivity: ε_s = 8.5–11.2 [–].

InP samples were doped by Se:

- crystalline surface orientations: [1 0 0] and [1 1 0];
- concentration of donor admixtures: $N_n = 10^{15}$ cm^{-3};
- mobilities of the carriers in the volume were: μ_n = 4200 cm^2/(V·s), μ_p = 160 cm^2/(V·s);
- the bandgap width: ΔE_G = 1.27 eV;
- resistivity: $\rho = 1.5 \cdot 10^4$ [Ω·m];
- permittivity: ε_s = 9.8 [–].

3.2.1. Surface potential research

The theoretical dependence is a complex one and only its numerical calculation is possible.

The example of the dependence for monocrystalline InP [1 1 0] is shown in Fig. 3. Potential U_s is in a.u. [–] because it is related to the average thermal energy of the electrons in room temperature.

The electrical parameters of the near-surface area were changed by means of an external electric field E_d, applied to the semiconductor perpendicular to the tested surface. This field was applied to the semiconductor by means of the so-called drift voltage U_d. The experimental dependence (Fig. 4) is similar in nature to the theoretical relationship (Fig. 3).

The similarity between the function and the experimental dependence results mainly from the fact that the external electric field, changing the concentration in the subsurface area, also changes the size of the surface potential. The acoustic method of determining the surface potential in a semiconductor uses the theoretical relationship $U_{\mathrm{AE}} = f(U_s)$ and the experimental relationship $U_{\mathrm{AE}} = f(U_d)$. On the experimental characteristics, the acoustoelectric voltage should be expressed in relative units, related to the value of acoustoelectric voltage at a zero drift field $\frac{U_{\mathrm{AE}}}{U_{\mathrm{AE}}(U_d=0)}$. In the point $U_d = 0$ [V], the relation $\frac{U_{\mathrm{AE}}}{U_{\mathrm{AE}}(U_d=0)} = 1$.

In the theoretical expression (Eqs (1) and (2)), the voltage is determined with accuracy to any multiplicative constant K. This constant should be selected so that the maximum on the theoretical characteristic and the maximum on the characteristic $\frac{U_{\mathrm{AE}}}{U_{\mathrm{AE}}(U_d=0)} = f(U_d)$ have this same value. Then, on the theoretical characteristic, it falls on the value corresponding to the surface potential in the semiconductor. The presented idea has been widely used in the study of surface potential in group III-V semiconductors.

GaP semiconductor crystal is a difficult research material for the acoustic method. This is due to the low mobility of charge carriers, as for the materials of group III-V, low concentration of carriers, and a wide energy gap. First of all, these properties of GaP make the phonon–electron interactions occurring in the piezoelectric waveguide-gallium phosphide system relatively weak. GaP research required special preparation of the test stand. To record the acoustoelectric signal, it was necessary to use an amplifier with a higher gain.

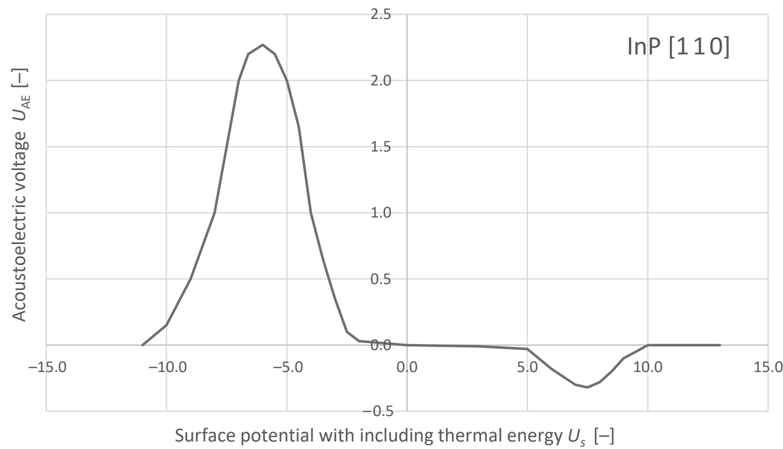

Fig. 3. Theoretical dependence of the transverse acoustoelectric tension U_{AE} on the surface potential U_s for InP [1 1 0] (a.u. – arbitrary units).

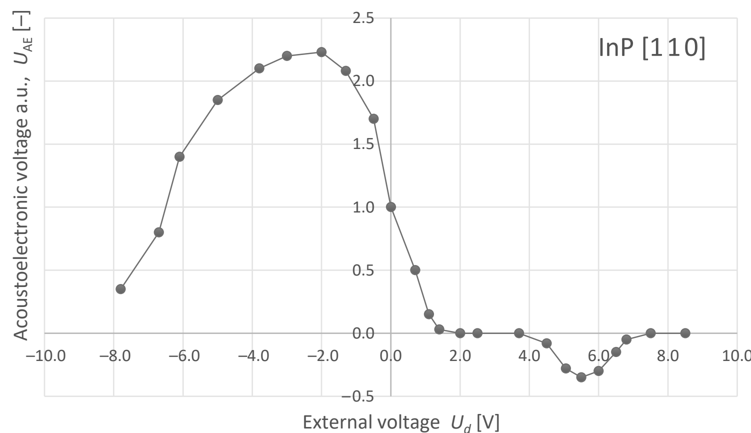

Fig. 4. Experimental dependence of the transverse acoustoelectric voltage U_{AE} as a function of the external drift voltage U_d (polishing with diamond paste).

Very careful signal shielding had to be provided. It was also necessary to shield the drift voltage source. GaP:Cr [1 0 0] tests with n-type conductivity were carried out. The tests were carried out at the frequency of 63 MHz. The surface potential for surfaces subjected to grinding with powders of various granulation as well as surfaces polished with diamond paste was investigated. Different clamping forces were used during machining. Grinding and chemical etching gave similar surface potential values after the treatment. It was noticed that in the GaP:Cr sample, after etching with HF acid and poorly washing the treated surface, the sign of the acoustoelectric voltage changed, after a few hours after the treatment, to the opposite. This suggests a change in the type of conductivity in the near-surface area. For the other tested materials of group III-V with electronic type of conductivity, no change in the sign of the effect from negative to positive was observed. The careful studies of the surface of GaP:Te doped gallium phosphide were also carried out (Fig. 5). Some of the results of the GaP studies are presented in (Pustelny *et al.*, 2008).

The values of the surface potential U_s were:

- HF acid etching – surface potential
$$U_s = -0.22 \pm 001 \text{ V};$$
- powder grinding 600 – surface potential
$$U_s = -0.20 \pm 001 \text{ V};$$
- polishing – surface potential
$$U_s = -0.17 \pm 001 \text{ V}.$$

It was noticed that the value of the U_s potential, as well as the size of the changes in the surface potential after the treatment on the surface exposed to the air atmosphere, is largely determined by the cleaning process of this surface. Washing in acetone, benzene or toluene after surface treatment often turns out to be insufficiently thorough.

For GaP crystals subjected to the benzene boiling process, after the surface treatment process, the surface sensitivity to external atmospheres is lower. The aging tests as a function of the time the sample remains in the air atmosphere after the surface treatment were also carried out. The changes in surface potential were observed for several hours after the GaP sample was surface treated. Figure 6 shows the results obtained for

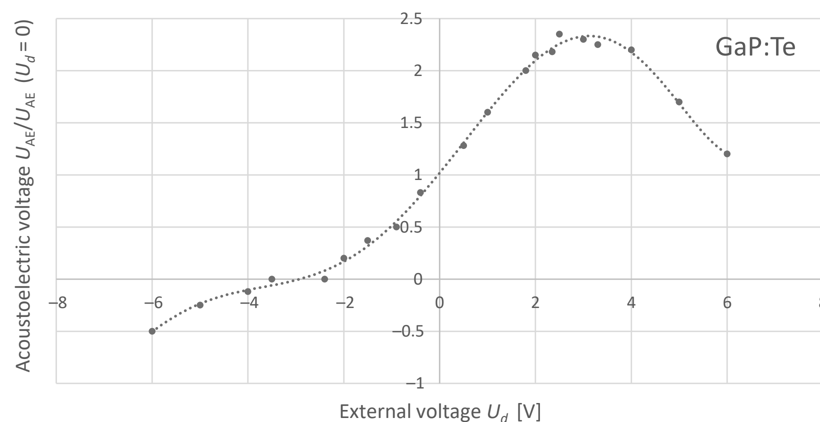

Fig. 5. Experimental dependence of transverse acoustoelectric voltage U_{AE} on external voltage U_d for GaP:Te [1 1 0] surface (Pustelny, Pustelny, 2009).

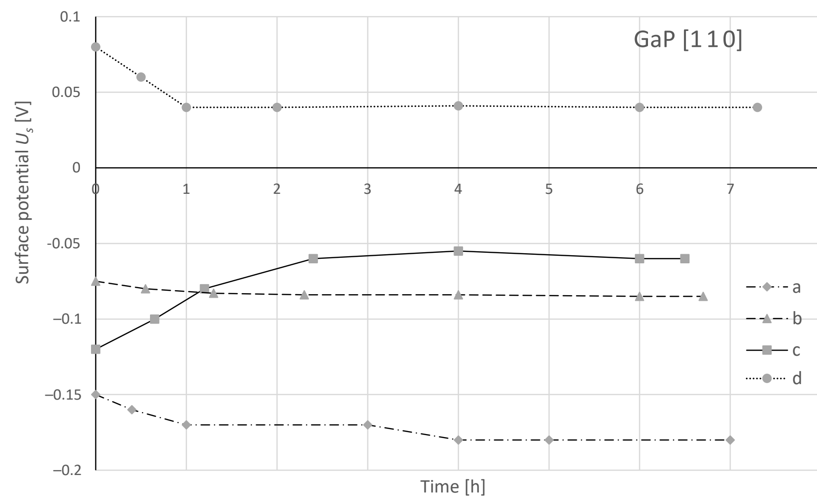

Fig. 6. Surface potential changes (presented in hours) for different surface treatments in intrinsic GaP [1 1 0]: a) grinding with corundum powders; b) polishing with diamond paste; c) digestion with HNO_3 acid; d) digestion with HF acid.

an undoped GaP [1 1 0] sample (GaP intrinsic type). The changes in the value of the surface potential U_s continued for about 2 hours after the surface treatment process. It has been noticed that these changes are strongly influenced by the process of washing the surface after its previous chemical and mechanical treatment.

It should be emphasized that the surface potential is an electric parameter very sensitive to the surface treatment method and the amount of water vapor in the air atmosphere. The research showed that the value of the electric surface potential and its sign are influenced, in addition to the surface treatment method, also by the concentration of charge carriers and the type of electrical conductivity of the semiconductor.

3.2.2. Effective lifetime of the charge carriers

Then the speed of recombination processes is characterized by the parameter – the effective lifetime of carriers. The lifetime of carriers (apart from the recombination rate) is the basic parameter characterizing the kinetics of recombination phenomena. As a result of the transverse acoustoelectric effect, the electric field associated with the surface wave causes a change in the distribution of the equilibrium concentration of carriers. The voltage quickly reaches its maximum value and then decreases exponentially. The decrease rate $U_{\mathrm{AE}} = f(t)$ results from the value of the effective lifetime of the charge carriers in the subsurface area. Based on the research of the time shape $U_{\mathrm{AE}}(t)$, an acoustic method for determining the effective life time of minority carriers in the near-surface area has been developed.

Life time studies of carriers in the subsurface area of a wide group of III-V semiconductors were carried out. Table 1 shows the test results of three different gallium phosphide single crystals. GaP:Te [1 1 0] and GaP:Cr [1 1 0] crystals were characterized by n-type electrical conductivity, while GaP [1 0 0] was of the intrinsic type. The influence of various surface treatments on the lifetime values of the charge carriers was investigated. Various methods of chemical treatment were also used.

Table 1. Life time of electrical carriers in GaP after different surface treatment.

	Semiconductor	Life time of carriers τ_{ef} [μs]		
		polishing	grinding	HP acid etching
1	GaP:Cr(n)	~1.0 ± 0.3	12 ± 3	24 ± 4
2	GaP (intrinsic)	5 ± 1	3 ± 1	3.5 ± 1.0
3	GaP:Te(n)	2.0 ± 0.1	2.2 ± 0.4	0.40 ± 0.04

Some life time values have been collected in Table 1. Life time values varies widely.

During the research, changes in the course of $U_{\mathrm{AE}}(t)$ were noticed, as well as changes in the lifetime value of τ_{ef} carriers depending on the residence time of the sample in the air atmosphere after its previous treatment. Extensive research was carried out on the effect of the sample residence time after surface treatment on the lifetime values of the charge carriers on the surface (so-called aging tests). Aging studies showed that after surface treatment of the samples, their τ_{ef} values changed while staying in the air atmosphere. Life time values were established after a few and sometimes even several hours. The differences between the values of τ_{ef} immediately after treatment and the fixed value were as high as twenty percent. The size of these differences strongly depended on the type of surface treatment.

For the InP:Se sample (n-type), research was carried out on the effect of chemical treatment in hydrofluoric acid, as well as research on the effect of grinding with grinding powders of different granulation and polishing with diamond paste on the life time τ_{ef}. For this semiconductor, the τ_{ef} values after various surface treatments changed from approximately 2 μs (for the ground sample) to approximately 4 μs for the surface etched in HF. For about 20 hours after the treatment, changes in the lifetime of the carriers were observed on the surface not protected against the action of the air atmosphere (Fig. 7). For the same semiconductor crystal, the surface aging time after the chemical treatment was significantly longer than after the mechanical treatment of this surface. During the tests, it was noticed that no changes of the aging type occurred in the sample placed immediately after treatment in deionized water. Life time τ_{ef} practically did not change (Fig. 7; N-characteristic).

3.2.3. Mobility of electric charge carriers in the near-surface area

The electrical conductivity of a semiconductor crystal, apart from the concentration of charge carriers (concentration of electrons and holes), is also determined by their mobility. The mobility of charge carriers is understood as the average speed that carriers acquire under the action of a unit external electric field. Electron mobility studies were carried out in monocrystalline GaP:Te [1 1 0] for various types of surface treatments. Figure 8 shows the changes of the acoustoelectric voltage amplitude on the surface wave power for a GaP crystal after various treatments of its surface. The characteristics of $U_{\mathrm{AE}} = f(P_s)$ show a linear relationship.

The results of GaP:Te [1 1 0] mobility studies are shown below ($U_d = 0$):

– after grinding with corundum powder
$$\mu = 75 \pm 10\ \mathrm{cm}^2/(\mathrm{V}\cdot\mathrm{s});$$
– after polishing with diamond paste
$$\mu = 120 \pm 10\ \mathrm{cm}^2/(\mathrm{V}\cdot\mathrm{s});$$
– after acid digestion HNO_3
$$\mu = 90 \pm 10\ \mathrm{cm}^2/(\mathrm{V}\cdot\mathrm{s});$$
– after acid digestion HF
$$\mu = 95 \pm 10\ \mathrm{cm}^2/(\mathrm{V}\cdot\mathrm{s}).$$

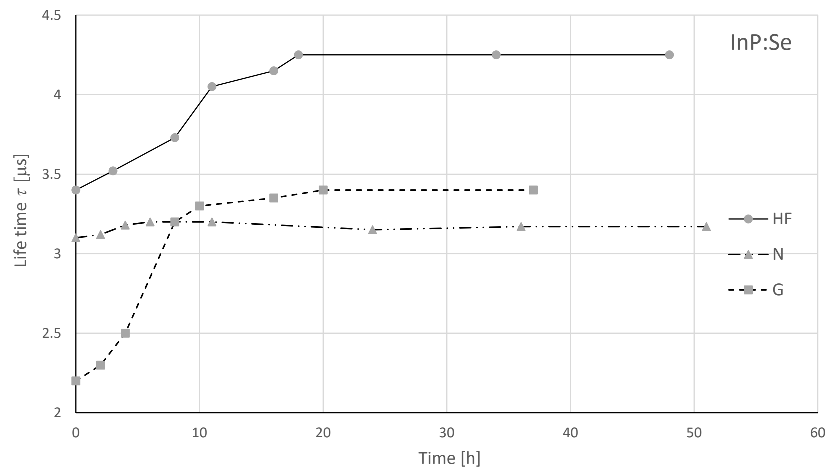

Fig. 7. Changes in the lifetime of carriers in InP:Se after different surface treatment:
HF – acid etching, G – grinding, N – long stay of the sample in deionized water (~20 h).

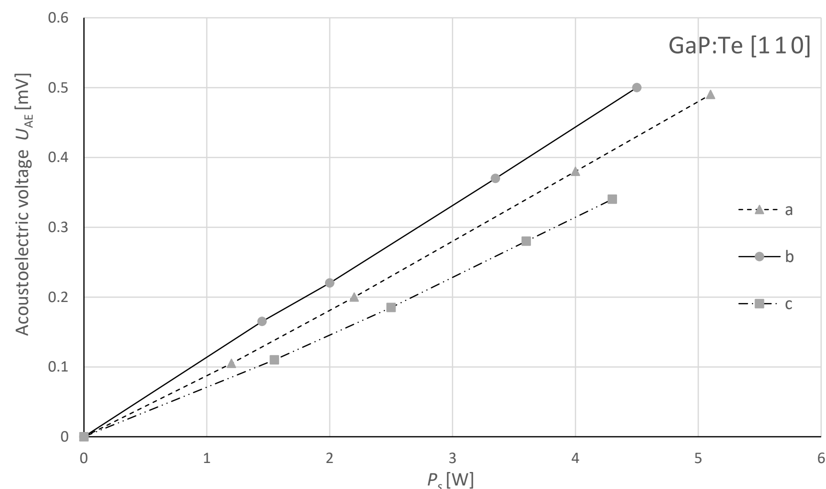

Fig. 8. Changes of U_{AE} amplitude as a function of SAW power P_s after different surface treatments (for $U_d = 0$): a) grinding with corundum powders; b) polishing with diamond paste; c) etching in HNO_3 acid.

The carrier mobility values for the surface undisturbed by the external field and for the surface to which the tension was applied, determined by the acoustic method, practically did not differ. This is mainly due to the fact that the tested semiconductor was a high-resistance material with a low concentration of carriers (electrons). The external electric field, to a degree irrelevant to the scattering processes, changed the concentration in the subsurface area. In the case of an electric field in the opposite direction (voltage), an inversion layer was formed on the GaP surface. The type of conductivity changed from electronic to hole. This was manifested in the change of the sign of the voltage from positive to negative. The estimated hole mobility for the inversion layer was approximately $\mu_p = 65\ \text{cm}^2/(\text{V}\cdot\text{s})$.

Figure 9 shows the dependence of the acoustoelectric voltage as a function of the surface wave power (at its 81 MHz frequency) for three different values of external voltages U_d, applied perpendicularly to the tested semiconductor surface. For the voltage applied perpendicularly to the tested surface, a weak enrichment area was formed on that surface, with increased electrical conductivity.

Figure 10 shows the dependence of the voltage amplitude on the wave power for InP:Se [1 1 0] crystals (at 72 MHz). The power of the surface wave is proportional to the square of the voltage U_{in} at the transmitting transducer: $P_r \sim U_{\text{in}}^2$.

The SAW power is expressed in contractual (arbitrary) units P_r, where the value $P_r = 10$ corresponds to the amplitude of high frequency voltage applied to the interdigital transducer at the value $U_{\text{in}} = 1$ V. Also on the ordinate axis, the acoustoelectric voltage is expressed in contractual units (a.u.) in such a way that the value $U_{\text{AE}} = 1$ [–] corresponds with $P_r = 10$ [–].

As shown the acoustoelectric effect in a wide range of surface wave power is linear – the magnitude of the transverse acoustoelectric voltage TAV is a linear function of the surface wave power.

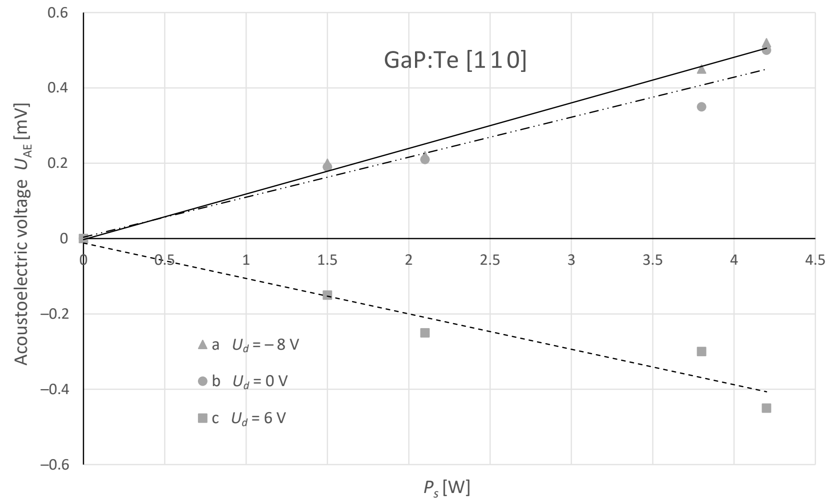

Fig. 9. Transverse acoustoelectric voltage as a function of surface acoustic wave power $U_{\mathrm{AE}} = f(P_s)$ for different polarization of U_d.

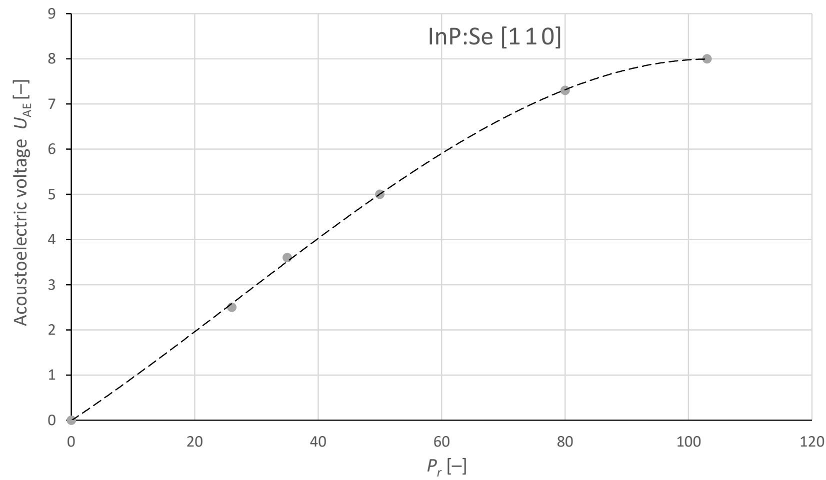

Fig. 10. Transverse acoustoelectric voltage as a function of surface acoustic wave power $U_{\mathrm{AE}} = f(P_r)$.

4. Measurement capabilities of the acoustoelectric method of testing surface of semiconductors

The accuracy of determining the parameters of the near-surface area with using the acoustoelectric method determines primarily on the accuracy of experimental results. The method uses both the results of experimental research and the results of theoretical analysis. The accuracies of the determination, using the acoustoelectric method developed, are of course influenced by the accuracy of the transverse acoustoelectric voltage measurement.

The test stand uses high-class devices: high-frequency signal generators for the generation of acoustic surface waves, signal generators in the synchronization and triggering path, measuring amplifiers and a high-class digital oscilloscope. This allowed for measurements of $U_{\mathrm{AE}}(t)$ acoustoelectric voltage with an accuracy of about 1–2%, depending on the intensity of acoustoelectric interactions in the tested sample. As has been shown, the idea of determining the value of the surface potential as well as the concentration of carriers and electrical conductivity in the subsurface area uses both the experimental relationship $U_{\mathrm{AE}}(t) = f(U_d)$ and theoretical dependencies of the acoustoelectric voltage as a function of semiconductor surface parameters. Although the theoretical analysis tried to take into account the different properties of the semiconductor surface as accurately as possible from its volumetric properties, the theoretical model of the phenomenon required some simplifications.

For example, it assumed that the interaction of the wave with the carriers leads to slight changes in the carrier concentration compared to the equilibrium ones. The presented analysis shows that this assumption is always properly fulfilled for the applied surface wave powers.

The method thus introduces a difficult for determination systematic error. The analysis of the theoretical expression for acoustoelectric voltage allows to determine the conditions under which the unknown systematic error is the smallest. The most accurate theoretical results are obtained for non-degenerate semiconductors with fully ionized dopants. This does not constitute a significant limitation of the method, as the experimentally tested semiconductors are characterized by high resistance and a relatively low concentration of carriers for which the condition of admixtures ionization at room temperature is met. The changes in the concentration of carriers in the near-surface area were included in the expression for the effective Debye radius, in the expression on the mobility of the carriers, and even in the expression for the dielectric permittivity of a semiconductor. The method uses some volume parameters, namely: the mobility of electrons and holes as well as the concentration of carriers in the volume. As a rule, this information is provided by the manufacturer of the semiconductor material. Otherwise, the application of the developed acoustic method would require additional supplementary measurements. In theoretical expressions, the author used the values of these volumetric parameters provided by producers of semiconductor crystals – the studied crystals were produced at the Institute of Physics of the Lviv University of Technology (Ukraine) and at the Institute of Electronic Materials Technology in Warsaw (Łukasiewicz Research Network, Poland).

As it results from the numerical analysis of the expression for transverse acoustoelectric voltage, in the case of carrier concentration n_s and electrical conductivity, the theoretical dependencies $U_{\mathrm{AE}} = f(n_s)$ and they have a maximum in a relatively wide range. Maxima are often blurred and occur in a wide range of changes in n_s and σ_s. The idea of the method of determining these parameters uses the comparison of theoretical characteristics: $U_{\mathrm{AE}} = f(\sigma_s)$ and the experimental characteristics of $U_{\mathrm{AE}}(t) = f(U_d)$. In particular, it is the maximum values on these characteristics that are compared. The function $U_{\mathrm{AE}} = f(U_s)$ usually has a maximum marked sharply. Therefore, the accuracy of the determination of the concentration and conductivity is much lower than the accuracy of the determination of the U_s potential. The analysis shows that the results of concentration and conductivity measurements may be burdened with uncertainty of up to ±20%: $\delta \underline{n}_s \approx \pm 20\%$ and $\delta \underline{\sigma}_s \approx \pm 20\%$.

The analyses show that the uncertainty of the determination of the surface potential did not exceed: $\delta \underline{U}_s \approx \pm 10\%$. In terms of testing these surface parameters, the accuracy is quite good. The field effect method allows to obtain results with better accuracy but for much lower frequencies. For frequencies of 100 MHz (and above), the use of the field effect method is very difficult (Wojas, 1995). The acoustic method does not make it possible to test semiconductors with too large concentrations and small concentrations. In these ranges, the interactions of the SAW with the charge carriers are small, often not measurable at all. For GaAs, GaP, and InP they are of the order of charge carrier concentration $n = 10^{18}$ cm^{-3} the acoustoelectric effect was not observed. This is undoubtedly a limitation of the developed method. The materials used as substrates for electronic technology are usually high-resistance materials and can therefore be tested using the acoustic method. Crystalline gallium phosphide GaP is a difficult material for research by means of the acoustoelectric effect method. This is due to the low mobility of electrons and holes as well as its wide band gap. Due to these properties, the acousto-electron interactions in GaP are relatively weak. Interpretation of the experimental results is difficult, and the accuracy of the determined parameters is lower than for other materials. The method of determining the mobility of carriers from the measurements $U_{\mathrm{AE}} = f(P_s)$ allows to study semiconductors with a monopolar type of conductivity, for which the influence of minority carriers on electrical conductivity can be neglected. The acoustic method of determining the mobility of carriers does not allow to distinguish the contribution of electrons and holes to the electrical conductivity in a bipolar semiconductor. Other electrical methods, such as the field effect method, also have limitations of this kind.

5. Conclusions

The conducted tests confirmed that the values of electrical and electron parameters of the near-surface area in crystalline semiconductors may significantly differ from the values of these parameters in the volume, provided by their manufacturer. It should also be emphasized that the values of these parameters significantly affect the mechanical and chemical procedure of the surface treatment.

The developed acoustoelectric method for determining the parameters of the subsurface area in semiconductors is a high-frequency method. Measurements were carried out in the frequency range from 30 to 300 MHz. There is a possibility of a significant extension of the frequency range (even up to GHz).

The method enables the determination of dynamic values of the tested surface parameters. With the need to produce electronic circuits with ever higher operating frequencies, dynamic measurements of the properties of the subsurface area of semiconductor materials after their surface treatments should be attractive for technology of electronic elements. The acoustoelectric method is a non-destructive method. It does not require a method of sample preparation for testing. It does not require placing ohmic contacts on the sample.

The process of making ohmic contacts is usually a technologically difficult process for group III-V semiconductors that requires vacuum sputtering of various metals and annealing of the semiconductor sample at high temperatures. As a result of these processes, the electrical and electronic properties in the near-surface area can change significantly compared to the initial properties. Changes difficult to quantify. No need to apply ohmic contacts in the tested semiconductor is an extremely important advantage of the developed acoustic method. An important and very advantageous property of the method is the fact that three parameters of the subsurface area: U_s, n_s, and σ_s are determined on the basis of one series of experimental results $U_{\mathrm{AE}} = f(U_d)$.

The new, high-frequency, non-destructive, acoustic technique for testing the real surface of semiconductors can be a valuable addition to the existing test methods.

As already mentioned, the intention of these studies were to show that acoustoelectric phenomena can be used in characterizing the properties of the subsurface area in crystalline semiconductors. A separate area of practical applications of acoustic surface waves of the Rayleigh type is sensorics, in particular the detection of a selected gas in air or a gas mixture. SAW sensors, including gas sensors, are commonly produced in a layer system: piezoelectric waveguide – sensor layers. The sensor layers are often based on semiconductor micro- and nanolayers. The sensor structures are also made of polymer semiconductors and organic semiconductors (Jakubik *et al.*, 2005; 2006; Hejczyk *et al.*, 2015; Pasternak *et al.*, 2020).

Structures on acoustic surface waves are also used in medical diagnostics and process chemistry – in chemical dosing microsystems and in microfluidics (Muhasincan *et al.*, 2015; Sesen *et al.*, 2014; 2015; 2017; Franke *et al.*, 2009; Ding *et al.*, 2012; Urbanczyk *et al.*, 2011; Jung *et al.*, 2016; 2017; Ha *et al.*, 2015; Yaralioglu, 2011; Schmid, Franke, 2013). The problems of sensors and actuators based on SAW in this paper were not analysed.

The development of semiconductor nanotechnology has caused interest in acoustoelectric effects at the quantum level – in phono-electron interactions. Scientific literature in the field of phonon-electron interactions is getting richer.

In the author's opinion, the following works deserve attention in the field of quantum acoustics: (Hanson *et al.*, 2007; Xiang *et al.*, 2013; Zhang, Xu, 2011; Ford, 2017; Barnes *et al.*, 2000; Biroun *et al.*, 2020a; 2020b). It can be expected that the practical applications of quantum acoustics will develop intensively in the near future.

To sum up, it should be recognized that the effects accompanying the propagation of surface acoustic wave in the layered structure: piezoelectric crystal – semiconductor layer, apart from the cognitive and physical aspects, also have important utilitarian considerations.

Acknowledgments

The Author would like to thank Dr Barbara Pustelny and also Michal Wilk, and Wojciech Trzaskalik for their help in conducting experimental and technological research works.

References

1. Auld B.A. (1973), *Acoustic Field and Waves in Solids*, Vol. 1, Wiley-Press INC, New York.

2. Barnes C.H.W., Shilton J.M., Robinson A.M. (2000), Quantum computation using electrons trapped by surface acoustic waves, *Physical Review B*, **62**(12): 8410–8419, doi: 10.1103/PhysRevB.62.8410.

3. Biroun M.H. *et al.* (2020a), Acoustic waves for active reduction of contact time in droplet impact, *Physical Review Applied*, **14**(2): 024029, doi: 10.1103/PhysRev Applied.14.024029.

4. Biroun H.M., Rahmadi M., Tao R., Torun H., Jangi M., Fu Y. (2020b), Dynamic behavior of droplet impact on inclined surfaces with acoustic waves, *Langmuir*, **36**(34): 10175–10186, doi: 10.1021/acs.langmuir.0c01628.

5. Bury P., Hockicko P., Rampton V.W. (2003), Acoustoelectric investigation of optically induced deep centers in GaAs/AlGaAs heterostructures, *Acta Physica Slovaca*, **53**(3): 189–194.

6. Ding X. *et al.* (2012), Standing surface acoustic wave (SSAW) based multichannel cell sorting, *Lab on a Chip*, 12(21): 4228–4231, doi: 10.1039/C2LC40751E.

7. Drewniak S. *et al.* (2013), Investigations of SAW structures with oxide graphene layer to detection of selected gases, *Acta Physica Polonica A*, **124**(3): 402–405, doi: 10.12693/APhysPolA.124.402.

8. Elhosni M. *et al.* (2016), Magnetic field SAW sensors based on magnetostrictive-piezoelectric layered structures: FEM modeling and experimental validation, *Sensors and Actuators A: Physical*, **240**: 41–49, doi: 10.1016/j.sna.2015.10.031.

9. Ford C.J.B. (2017), Transporting and manipulating single electrons in surface-acoustic-wave minima, *Physica Status Solidi B*, **254**(3): 1600658, doi: 10.1002/pssb.201600658.

10. Franke T., Abate A.R., Weitz D.A., Wixforth A. (2009), Surface acoustic wave (SAW) directed droplet flow in microfluidics for PDMS devices, *Lab on a Chip*, **9**(18): 2625–2627, doi: 10.1039/B906819H.

11. Gulyaev Y.V. (2005), Acoustoelectronics (historical review), *Physics–Uspekhi*, **48**(8): 847–855, doi: 10.1070/PU2005v048n08ABEH002840.

12. Gustafsson M.V., Aref T., Kockum A.F., Ekstrom M.K., Johansson G., Delsing P. (2014), Propagating phonons coupled to an artificial atom, *Science*, **346**(6206): 207–211, doi: 10.1126/science.1257219.

13. Ha B.H. *et al.* (2015), Acoustothermal heating of polydimethylsiloxane microfluidic system, *Scientific Reports*, **5**: 11851, doi: 10.1038/srep11851.

14. Hanson R., Kouwenhoven L.P., Petta J.R., Tarucha S., Vandersypen L.M.K. (2007), Spins in few-electron quantum dots, *Reviews of Modern Physics*, **79**(4): 1217–1265, doi: 10.1103/revmodphys.79.1217.

15. Hejczyk T., Pustelny T. (2020), Analysis of the SAW system with the PANI + nafion sensing structure for detection of low concentration carbon monoxide, *Archives of Acoustics*, **45**(4): 681–686, doi: 10.24425/aoa.2020.135274.

16. Hejczyk T., Urbanczyk M., Pustelny T., Jakubik W. (2015), Numerical and experimental analysis of the response of a SAW structure with WO_3 layers on action of carbon monoxide, *Archives of Acoustics*, **40**(1): 19–24, doi: 10.1515/aoa-2015-0003.

17. Hermelin S. *et al.* (2011), Electrons surfing on a sound wave as a platform for quantum optics with flying electrons, *Nature*, **477**(7365): 435–438, doi: 10.1038/nature10416.

18. Holmes P.J. (1987), *The Electrochemistry of Semiconductors*, Academic Press INC, New York.

19. Jakubik W., Urbanczyk M., Cular S., Bethanabolta V. (2006), Acoustoelectric effect in Surface Acoustic Wave gas sensors (SAW) with metal – free phthalocyanine and palladium sensing bi-layers, *ECS Transactions*, **1**(19): 1–9.

20. Jakubik W.P., Urbanczyk M., Maciak E., Pustelny T., Stolarczyk A. (2005), Polyaniline thin films as a toxic gas sensors in SAW system, *Journal de Physique IV France*, **129**: 121–124, doi: 10.1051/jp4:2005129026.

21. Jung J.H., Desteer G., Ha B., Park J., Sung H.J. (2016), On-demand droplet splitting using surface acoustic waves, *Lab on a Chip*, **16**(17): 3235–3243, doi: 10.1039/C6LC00648E.

22. Jung J.H., Destgeer G., Park J., Ahmed H., Park K., Sung H.J. (2017), On-demand droplet capture and release using microwell-assisted surface acoustic waves, *Analytical Chemistry*, **89**(4): 2211–2215, doi: 10.1021/acs.analchem.6b04542.

23. Kapelewski J., Lila B. (2011), Elastic wave behaviour in 2-D acoustic interface superlattices of an altered phase, *Archives of Acoustics*, **36**(3): 603–611.

24. Macinnes A. *et al.* (1993), *Surface Passivation for III-V Semiconductor*, NASA Material Research Society, **4**(1).

25. Many A., Goldstein Y., Grover N.B. (1979), *Semiconductor Surfaces*, Nord Holland Press INC, Amsterdam.

26. Muhasincan S., Alan T., Neild A. (2015), Microfluidic plug steering using surface acoustic waves, *Lab on a Chip*, **15**(14): 3030–3038, doi: 10.1039/C5LC00468C.

27. Pasternak M., Jasek K., Grabka M., Borowski T. (2020), Surface acoustic wave interaction with a mixture of oxygen and nitrogen, *Archives of Acoustics*, **45(**3): 483–486, doi: 10.24425/aoa.2020.134065.

28. Peka G. (1987), *Physics of Semiconductor Surfaces* [in Ukrainian], Kiev University Press, Ukraine.

29. Pustelny B., Pustelny T. (2009), Transverse acoustoelectric effect applying in surface study of GaP:Te(111), *Acta Physica Polonica A*, **116**(3): 383–384, doi: 10.12693/APhysPolA.116.383.

30. Pustelny T. (1995), Acoustic method of investigating the surface potential in semiconductors. Study of the GaP:Te (110) real surface, *Ultrasonics*, **33**(4): 289–294, doi: 10.1016/0041-624X(94)00040-V.

31. Pustelny T. (1997), Surface acoustic wave techniques for the real-surfaces investigations of InP (111), InAs (111) semiconductors, *Acta Acustica united with Acustica*, **83**(3): 482–488.

32. Pustelny T. *et al.* (2013), The sensibility of resistance sensor structures with graphene to the action of selected gaseous media, *Bulletin of the Polish Academy of Sciences: Technical Sciences*, **61**(2): 293–301, doi: 10.2478/bpasts-2013-0027.

33. Pustelny T., Opilski A., Pustelny B. (2008), Determination of some kinetic parameters of fast surface states in silicon single crystals by means of surface acoustic wave method, *Acta Physica Polonica A*, **114**(6): A183–A190, doi: 10.12693/APhysPolA.114.A-183.

34. Pustelny T., Pustelny B. (2006), The acoustic method of investigating the electrical carrier mobility of the real GaP:Te (110) surface, *Journal de Physique IV France*, **137**: 223–226, doi: 10.1051/jp4:2006137046.

35. Pustelny T., Pustelny B. (2008), The acoustic method of the surface potential investigation in GaP:Te (110) real surface, *The European Physical Journal: Special Topics*, **154**(1): 281–284, doi: 10.1140/epjst/e2008-00561-x.

36. Red O., Snitko V. (1994), *Problems of Semiconductor Surface Physics* [in Ukrainian], Scientific Press, Kiev, Ukraine.

37. Rotter M., Wixforth A., Govorov A.O., Ruile W., Bernklau D., Riechert H. (1999), Nonlinear acoustoelectric interactions in $GaAs/LiNb0_3$ structures, *Applied Physics Letters*, **75**(7): 965–967, doi: 10.1063/1.124568.

38. Samulionis V., Banys J., Vysochanskij Y. (2004), Acoustoelectric effects in $Sn_2P_2S_6$-type ferroelectric semiconductors, *Physica Status Solidi (A)*, **201**(9): 2143–2147, doi: 10.1002/pssa.200406821.

39. Schmid L., Franke T. (2013), SAW-controlled drop size for flow focusing, *Lab on a Chip*, **13**(9): 1691–1694, doi: 10.1039/C3LC41233D.

40. Sesen M., Alan T., Neild A. (2015), Microfluidic plug steering using surface acoustic waves, *Lab on a Chip*, **15**(14): 3030–3038, doi: 10.1039/C5LC00468C.

41. Sesen M., Devendran C., Malikides S., Alan T., Neild A. (2017), Surface acoustic wave enabled pipette on a chip, *Lab on a Chip*, **17**(3): 438–447, doi: 10.1039/C6LC01318J.

42. Sesen M., Tunacay A., Neild A. (2014), Microfluidic on-demand droplet merging using surface acoustic waves, *Lab on a Chip*, **14**(17): 3325–3333, doi: 10.1039/C4LC00456F.

43. Sze S.M. (1995), *Physics of Semiconductor Devices*, John Wiley and Sons Inc., New York.

44. Tabib-Azar M. (1998), Characterization of electrical properties of semi-insulating GaAs using acoutoelectric voltage spectroscopy, *Solid-State Electronics*, **31**(7): 1197–1204, doi: 10.1016/0038-1101(88)90279-1.

45. Urbańczyk M. (2011), Analytical model of a SAW gas sensor, *WIT Transactions on Modelling and Simulation*, **51**: 483–494, doi: 10.2495/CMEM110431.

46. Urbaczyk M., Maciak E., Gut K., Pustelny T., Jakubik W. (2011), Layered thin film nanostructures of Pd/WO_{3-x} as resistance gas sensors, *Bulletin of the Polish Academy of Sciences: Technical Sciences*, **59**(4): 401–407, doi: 10.2478/v10175-011-0048-4.

47. Vanneste J., Buhler O. (2011), Streaming by leaky surface acoustic waves, *Proceedings of the Royal Society A: Mathematical, Physical and Engineering Sciences*, **467**(2130): 1779–1800, doi: 10.1098/rspa.2010. 0457.

48. Weisbuch C., Vinter B. (1991), *Quantum Semiconductor Structures*, Academic Press Inc., Boston.

49. Wojas J. (1995), *Physics of Semiconductors Surface* [in Polish: Fizyka powierzchni półprzewodników], Akademicka Oficyna Wydawnicza, Warszawa.

50. Wolf H.F. (1979), *Semiconductors*, John Wiley and Sons Inc., New York.

51. Xiang Z.L., Ashhab S., You J.Q., Nori F. (2013), Hybrid quantum circuits: Superconducting circuits interacting with other quantum systems, *Reviews of Modern Physics*, **85**(2): 623–653, doi: 10.1103/revmodphys.85.623.

52. Yaralioglu G. (2011), Ultrasonic heating and temperature measurement in microfluidic channels, *Sensors and Actuators A: Physical*, **170**(1–2): 1–7, doi: 10.1016/j.sna.2011.05.012.

53. Zhang S.H., Xu W. (2011), Absorption of surface acoustic waves by graphene, *AIP Advances*, **1**(2): 022146.

54. Zhu J., Popovics J.S., Schubert F. (2004), Leaky Rayleigh and Scholte waves at the fluid-solid interface subjected to transient point loading, *The Journal of the Acoustical Society of America*, **116**(4): 2101–2110, doi: 10.1121/1.1791718.